GLOBAL OCEAN SURFACE VECTOR WIND OBSERVATIONS FROM SPACE

(**R.F. Milliff [1], M.H. Freilich [2], W.T. Liu [3], R. Atlas [4], and W.G. Large [1]**)

[1] *National Center for Atmospheric Research, Boulder, Colorado*
[2] *Oregon State University, Corvallis, Oregon*
[3] *NASA Jet Propulsion Laboratory, Pasadena, California*
[4] *NASA Goddard Space Flight Center, Greenbelt, Maryland*

ABSTRACT **–** The global ocean surface vector wind is a key climate and operational observation, achievable from proven space-borne scatterometer systems. Science and operational requirements for sampling frequency, record length, spatial resolution, and global coverage are described in a climate context, using explicit examples in physical oceanography and air-sea interactions. A loosely coordinated assemblage of planned scatterometer missions from international space agencies in Europe, Japan, and the United States will span the next decade and beyond. The combined capabilities of these missions are projected to be sufficient to meet the science and operational requirements. The OCEANOBS community is urged to support scatterometer mission plans, and to strengthen international cooperation. A sensible means must be sought to transition scatterometry from research to operational agencies, while preserving the continuity and quality of a long data record.

1 - INTRODUCTION

Knowledge of surface vector winds over the oceans is essential for a range of oceanographic, meteorological, and climate investigations, as well as for improving regional and global operational weather prediction. Measurement techniques using satellite-borne active microwave scatterometers have been developed, tested, and refined over the past three decades. All-weather satellite vector wind measurements have been acquired and applied in a wide range of studies, leading to increased understanding of the measurement requirements and the impacts of sampling and resolution (in addition to instantaneous measurement accuracy) on the scientific and operational utilities of the data sets. The data obtained from the European Space Agency (ESA) ERS-1, 2 and NASA NSCAT scatterometers establish the foundation for continuous ocean surface vector wind measurements for the operational and application communities; and the frequently sampled, high resolution, multi-decadal time series of ocean forcing and air-sea fluxes required by the ocean, atmosphere, and climate research communities. Present plans call for flights of several microwave scatterometers (often several simultaneously) by U.S., European, and Japanese space agencies. However, the planned scatterometer missions are only loosely coordinated. No single polar-orbiting instrument can provide vector wind measurements with sufficiently high resolution, extensive coverage, and frequent sampling, nor can any single instrument be expected to operate for the long period needed to acquire climate-relevant time series. It is, therefore, essential that the ocean research and operational meteorological communities develop firm and realistic plans for ensuring the acquisition of the required high quality vector wind measurements in the coming decades, as well as plans for developing and evaluating improved, refined, and/or more cost-effective spaceborne measurement techniques.

This position paper outlines the scientific importance of all-weather ocean surface vector wind measurements, and quantifies the required characteristics of these measurements in the context of key ocean and climate prediction investigations and operational weather forecasting applications. The present "state of the art" in measurement technique is summarized, along with international plans for acquiring all-weather ocean vector wind data through the next decade. While spaceborne measurement of ocean surface wind velocity is technically challenging, active microwave scatterometry is a mature and tested approach which can satisfy science requirements with a coordinated set of missions. Other approaches (e.g., polarimetric microwave radiometry or bistatic analysis of GPS signal scattering from the ocean surface) have great promise and are being pursued in the research and development stages, but have yet to be tested in space.

The surface vector wind is a key variable in estimating the exchanges of momentum (kinetic energy) between the atmosphere and ocean. Surface wind speed is key in estimating fluxes of heat, longwave radiation, and moisture across the interface. Long-term, high-quality surface vector wind data sets are required to quantify air-sea fluxes such that energy balance budgets for the interactive Earth climate system can be obtained. Clearly, the surface vector wind is a key variable for development of, validation of, and eventually assimilation in, coupled climate model integrations.

The global ocean surface vector windfield is observable from space at near-mesoscale resolution. At this resolution, the surface vector windfield is an indicator of large-amplitude turbulent mixing events in the boundary layers of the atmosphere and ocean that can lead to deep convection in both fluids. We will demonstrate that resolving the episodic, large-amplitude events of these kinds poses significant challenges, but has large potential pay-offs in our abilities to quantify, model, and forecast the climate system.

Probably because the surface vector wind field occurs at the upper and lower boundaries of the ocean and atmosphere, its importance in climate issues for both fluids has yet to receive attention comparable to remote sensing data sets that address the fluid interiors (*e.g.*, altimetry, out-going longwave radiation). The experience gained from pioneering scatterometer missions (*e.g.*, SeaSAT, ERS-1, 2, and NSCAT) is expanding the appreciation in the climate community for the importance of accurate, global ocean, surface vector wind data.

Perhaps what is most noteworthy for OCEANOBS 99 is that the conjunction of research and technology that is emerging from spaceborne scatterometry and altimetry has brought us within sight of a significant milestone in the history of ocean observations. We are on the threshold of obtaining simultaneous global observations of the time and space scales in the surface vector winds and the ocean mesoscale eddy field that will allow us to address fundamental issues of direct vs.

indirect driving of the mesoscale eddies, and the conditions for strong turbulent mixing events in the ocean and atmospheric boundary layers.

2 - SCIENCE REQUIREMENTS

In an appendix we describe in some detail, large-amplitude geophysical events on various time and space scales that have climatic impacts and are within range of emerging technologies in active scatterometer systems for observing the ocean surface wind field. The physical processes include:

- inertial resonance and ocean mixing in mid-latitudes;
- diurnal cooling, ocean convection, and vertical mixing in the tropics;
- localized coastal upwelling along ocean eastern boundaries;
- eastern boundary wind-stress curl and sub-tropical gyre dynamics;
- wind-stress curl intermittency and the propagation of atmospheric storms;
- interannual forcing and western boundary current separation.

These examples help define temporal and spatial sampling requirements for the ocean surface vector wind observing system. These are summarized in the following table.

<u>Science Requirements</u>

Timescales	*Ocean Climate Processes*
inertial period (mid-latitudes)	vertical mixing inertial resonance
diurnal cycle (equator)	seasonal air-sea heat fluxes
autocorrelation timescale (coastal)	upwelling
first baroclinic mode Rossby wave basin scale transit time	western boundary current variability
ENSO	large-amplitude perturbations

Spatial Scales	
ocean mesoscale eddy field	mixing poleward transports feedbacks to the general circulation
boundary wind-stress curl	upwelling gyre morphology

Table 1

The highest frequency requirements are set by the inertial period timescale in mid-latitudes and the diurnal timescale at the equator. Global inertial timescale resolution is probably too expensive to achieve. However, a coordinated system of space-borne surface vector wind sensors could resolve segments of the same local inertial period (*e.g.*, with 3-hourly observations) for a finite time interval in the morning on ascending orbits, and again at night on descending orbits. Temporal sampling of this density might occur every other day for a given mid-latitude location.

Record length requirements are set by the importance of continuous, high-quality records over the life-cycles of large-amplitude climate scale perturbations. For example, consider the value of high-quality surface vector wind records for the initiation, maturation, and decay phases of individual ENSO events. Also, important western boundary current variability and water mass distributions are functions of basin-scale Rossby wave dynamics, requiring several years to propagate across basins of the world ocean. Record lengths on the order of a decade are required.

The highest wavenumber requirements result from the need to resolve wind-forcing on scales corresponding to the ocean mesoscale and eastern ocean boundary wind-stress curl features. The prospect of resolving, over large regions of the world ocean, the spatial scales of the surface wind field comparable to the mesoscale eddies marks a significant milestone in the short history of surface vector wind observations from space. Fundamental questions of direct vs. indirect forcing of the mesoscale eddy field can begin to be addressed by region, and by season. The feedbacks of the eddy circulation onto the mean flow can then begin to be quantified and parameterized in modern coupled climate simulations. Spatial resolution of the surface wind field at not coarser than 25*km* resolution is required.

The lowest wavenumber constraints for surface vector wind observations have to do with the consistent global representations of propagating and evolving atmospheric storm systems. The seasonal and regional integrals of these systems contribute to global budgets of heat, momentum, and moisture exchanges between the atmosphere and ocean that drive the climate system. Global coverage on the order of a day is required.

Thus, within the context of the problems identified above and described in more detail in the appendix, a set of measurement requirements was developed based on existing knowledge of the processes and of the scales of variability of the wind forcing fields. Although full understanding of the processes and true forcing do not exist, the notional science requirements are likely to yield a measurement set that will significantly advance scientific investigations given the existing technical and fiscal realities. A decadal, global ocean vector wind data set with the characteristics identified will fundamentally impact research by:

- Illuminating the relative importance of wind forcing in determining, diagnosing, and predicting climate change;
- Defining wind variability simultaneously on both small and large space and time scales that have not hitherto been quantitatively measured; and
- Providing a consistent wind forcing data set to test, constrain, and guide future theoretical and modeling investigations.

3 - PLANNED SCATTEROMETER MISSIONS

The capabilities of planned ocean surface vector wind measurement missions and instruments are examined in light of the science requirements.

Three space borne vector wind measurement systems are proposed in the 1999-2012 time period:

- Broad-swath, dual-pencil beam active Ku-band scatterometers (*e.g.*, SeaWinds);
- Dual-swath, 3-look active C-band scatterometers (*e.g.*, ASCAT); and
- Dual- and single-look passive polarimetric radiometers (*e.g.*, WINDSAT, CMIS).

The timeline for past, existing, and planned vector wind measurement missions is shown in the following chart.

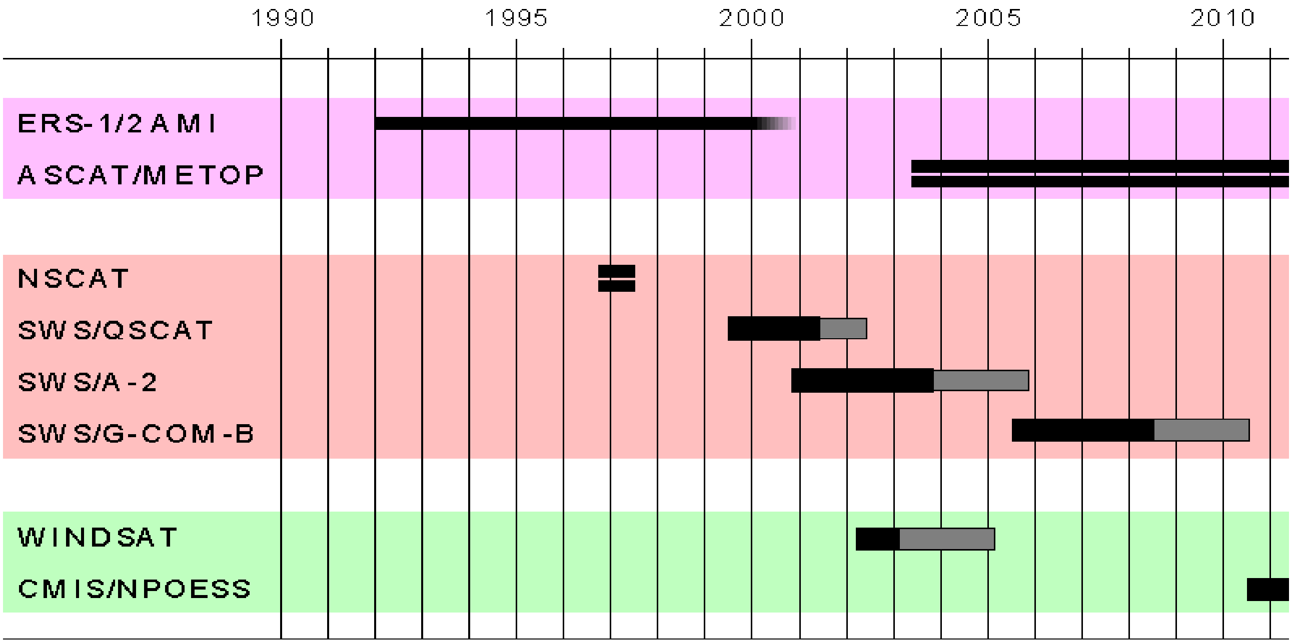

Figure 1. Past, existing, and planned surface vector wind space craft missions.

These systems provide different vector wind measurement accuracies, different spatial and temporal resolutions of the instantaneous surface wind field, as well as different global coverages.

Accuracy requirements for the surface vector wind for climate purposes are on the order of ± 1 m s^{-1} for wind speed, and a directional accuracy such that long-term average wind-stress curl is accurate to within 1×10^{-8} N m^{-3}. The existing spatial resolution for the ERS-2 system is *O* (50*km)*. Anticipated spatial resolutions range from *O* (12*km)* (*e.g.*, SeaWinds class instruments) to *O(*25*km)* (*e.g.*, ASCAT). The swath configurations are represented in the chart (Fig. 1). The SeaWinds instruments span up to 1800*km*, with no nadir gap. The ASCAT sampling is similar to that of NSCAT. ASCAT will have two, 550*km* wide swaths separated by a 660*km* wide gap centered on the subsatellite track. The polarimetric systems (WINDSAT and CMIS) have yet to be tested in space, under a wide variety of environmental conditions.

The temporal resolution requirements present the greatest challenge for future vector wind measurement data sets. The near-polar orbits and swath measurement patterns result in irregular space-time sampling at any surface location. There is no single metric with which to completely characterize the coverage of either single or multiple instruments, and production of gridded fields from the irregularly sampled data will require interpolation between measurements (*e.g.*, Chin *et al.*, 1998). Figure 2 demonstrates the global ocean coverages for existing and planned scatterometer missions based on simulations performed using the orbit and swath parameters described above.

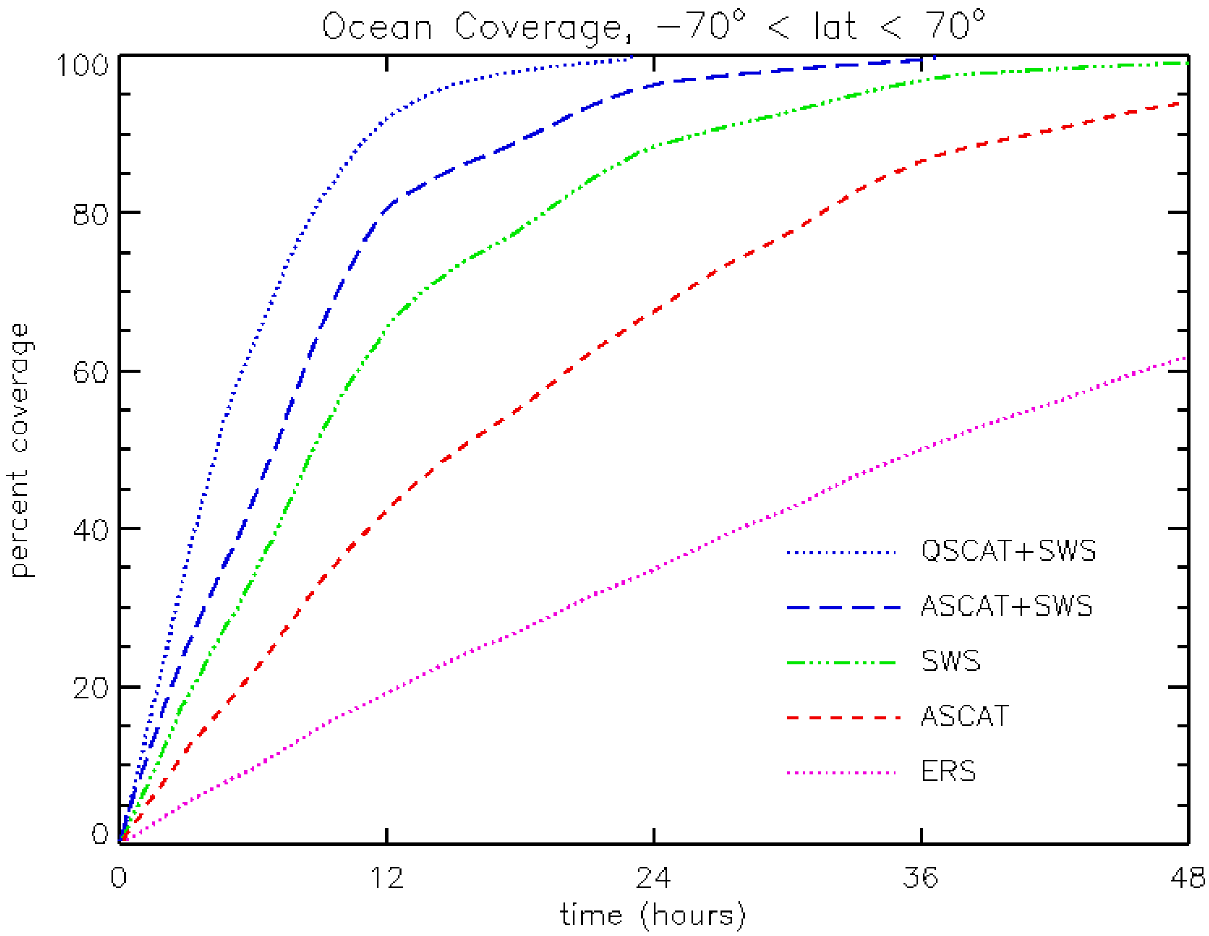

Figure 2. Total global coverage vs. time for current and planned scatterometer missions. "ERS," "ASCAT," and "SWS" represent single-instrument coverages for ERS single-swath, ASCAT dual-swath, and SeaWinds broad swath coverage, respectively. "ASCAT + SWS" represents coverage achieved from co-orbiting ASCAT and SeaWinds instruments on the Envisat and ADEOS-2 missions, respectively; "QSCAT + SWS" represents coverage from co-orbiting SeaWinds instruments on the QuicSCAT and ADEOS-2 missions.

It is clear that the tandem QuikSCAT and ADEOS-2 missions (both with broad-swath SeaWinds instruments) sample more than 90% of the ice-free oceans in 12 hours, resolving the diurnal cycle over the vast majority of the world ocean.

Examination of sampling intervals as a function of geographic location provides basic information on the temporal resolution of point wind time series, and indicates the quantity of auxiliary statistical information necessary to construct an accurate vector wind time series at a specific point. Sampling simulations were analyzed to determine sampling interval distributions at points on a 2° × 2° grid extending from the equator to 60°N latitude and spanning 80° of longitude. Mean sampling intervals were calculated at each grid location in the domain, and the mean sampling intervals were zonally averaged. Results for the single and tandem missions are shown in Fig. 3.

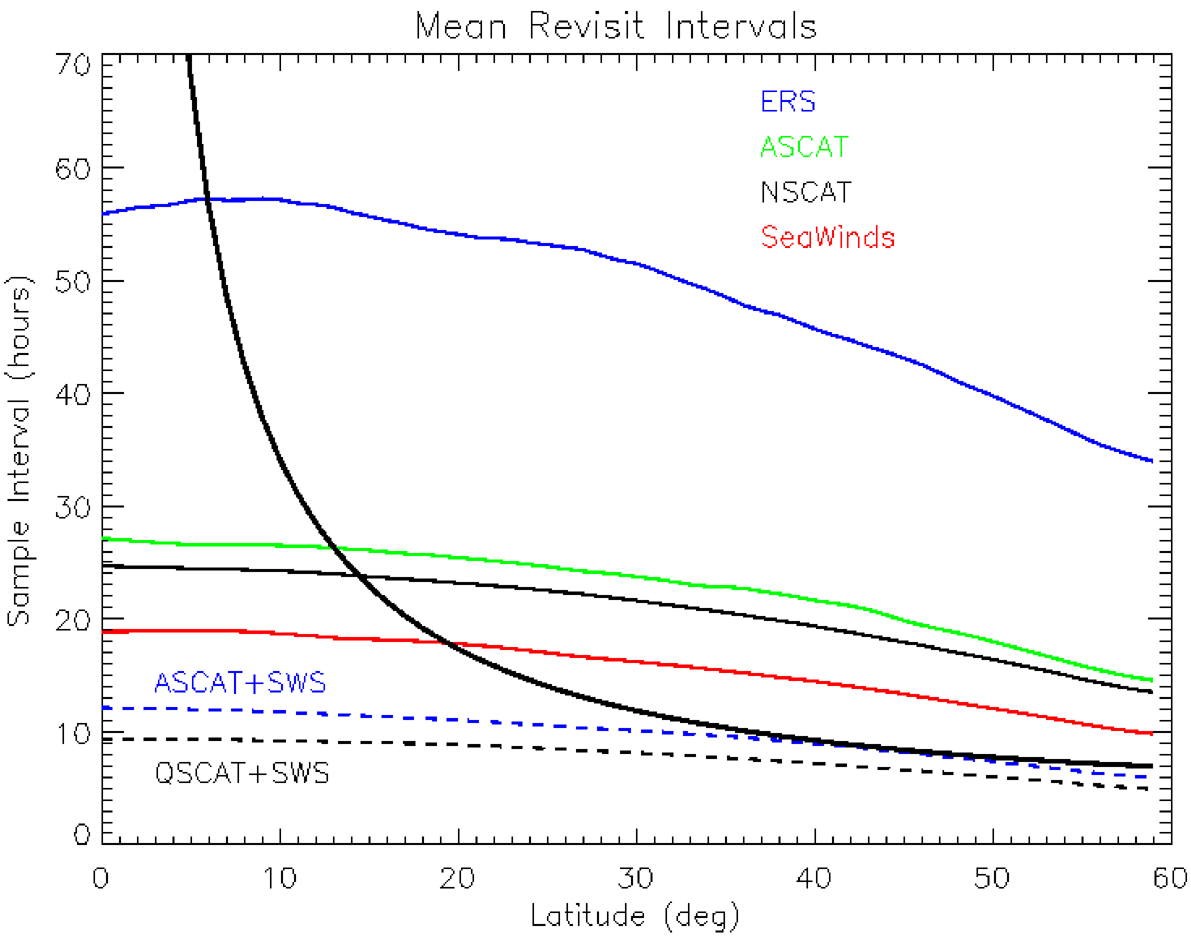

Figure 3. Mean time between samples vs. Latitude (at each location) for current and planned scatterometer missions. Single and tandem mission designations as in Figure 2 ("NSCAT" represents the dual-swath NSCAT instrument on the ADEOS-1 mission).

As expected, mean sampling intervals are markedly lower for the tandem mission periods. The thick black line decreasing like $\sin^{-1}\phi$ (where ϕ is latitude) denotes the sampling interval required to resolve the inertial period. The tandem mission periods for ASCAT+SeaWinds and SeaWinds+SeaWinds will allow resolution of the inertial period at all latitudes, and resolution of the diurnal cycle in the tropics.

4 - OPERATIONAL APPLICATIONS OF SURFACE VECTOR WIND FIELDS

The lack of adequate observational data has long been recognized as a major factor limiting weather forecasting skill. Numerical weather prediction (NWP) models require the complete specification of the initial value of the model variables, yet only a fraction of the required initial data are available at any given time. The required data consist of the three-dimensional fields of temperature, humidity, and horizontal velocity at locations comparable in spatial distribution with the grid points of the model used. Most of the data obtained by conventional ground-based methods are provided at the so-called synoptic times, 0000, 0600, 1200, and 1800 GMT. Numerical forecasts are performed at operational centers every day from 0000 and 1200 GMT initial conditions. The conventional data available at synoptic times fall far short of being sufficient in number or coverage. Thus, the use of space-based measurements offers an effective way to supplement the conventional synoptic network. Ocean surface winds measured by satellite can provide initial state and verification data for NWP models and local weather and wave forecasting. There are two primary ways in which satellite surface wind data can improve NWP model forecasts. First, they can contribute to improved analyses of not only the surface wind field, but through the data assimilation process, to an improved representation of the atmospheric mass and motion fields in the free atmosphere above the surface as well. In addition, the satellite surface wind data in conjunction with other satellite observations (cloud-track winds and temperature and water vapor profiles) can provide the data necessary to improve model formulations of the planetary boundary layer, as well as other aspects of model physics. In so doing, two of the major sources of error for NWP could be reduced, thereby yielding improved short-range forecasts over the oceans, and improved extended-range forecasts over both the oceans and continental areas.

Currently, satellite surface wind data are used to improve the detection of intense storms over the ocean, as well as to improve the overall representation of the wind field in NWP models. As a result, these data are contributing to improved warnings for ships at sea and to improved global weather forecasts. The results of global data assimilation experiments routinely show improvements in the location and intensity of cyclones and fronts over the oceans (*e.g.* Atlas *et al.*, 1999). NSCAT data were incorporated into the GOES Data Assimilation System improving cyclone positions by distances on the order of 500*km* (Atlas and Hoffman, 1999). The resulting improvement to numerical weather forecasts is typically large and significant in the Southern Hemisphere. In the Northern Hemisphere the impact on numerical forecasts is smaller on average, but on occasion significant improvements to the predicted intensity and location of storms occur.

5 - SUMMARY AND RECOMMENDATIONS

Teams of researchers, engineers, and operational practitioners have streamlined and strengthened their interactions in using and developing ocean surface vector wind data sets from space-borne observing systems. A proven track record for international cooperation exists (*e.g.,* between ESA, the Japanese Space Agency, and NASA), with substantial interest in future collaborations. The maturation of novel *in-situ* calibration technologies is proceeding apace. All of these assets are appropriately applied to the validation of new scatterometer technologies, and to the eventual transition to operational missions of a global ocean surface vector wind observing system.

Development and deployment costs for the recent QuikSCAT mission (launched June 1999) were under $*100M*, with about half going to the launch vehicle. The turnaround time from project start to instrument turn-on in space was on the order of 1 year. The QuikSCAT mission is the fastest and cheapest development and deployment to date in the NASA Earth Science Enterprise. The QuikSCAT mission sets a standard in these regards for future scatterometer missions in the transition to an operational surface vector wind observing system. The QuikSCAT mission marks the first in a planned sequence of overlapping, broad-swath, scatterometer missions to by launched and supported by the international community (Fig. 1). The climate research and operational communities are encouraged to endorse the planned international efforts, and to defend the overall plan as necessary in the future.

All existing spaceborne ocean surface data sets having extensive and frequent sampling, relatively stable accuracy, and decadal-scale time series length have been achieved through flights on multiple, operational missions (*e.g.* wind speed from SSM/I microwave radiometers on the DMSP spacecraft, and clear-sky sea-surface temperatures from AVHRR on POES missions). Such operational systems and missions are characterized by: clear, comprehensive, and stable requirements with at least one demonstrated measurement approach that satisfies the requirements; a need for continuous and long-term measurements processed and delivered in near-real-time for at least some applications (*e.g.* weather forecasting); and often the need for multiple co-orbiting spacecraft or instruments to meet sampling requirements. All-weather measurement of ocean surface vector winds has been proven by direct spaceborne demonstration in research missions. The requirements to ensure basic measurement utility for research applications are understood and have been summarized above. The challenge for the ocean observations community is to craft a means by which the vector wind measurement techniques, proven on research-oriented satellite missions, can be transitioned to operational missions and programs, while preserving the integrity of the future measurements and the continuity of the data set.

6 - APPENDIX

We present here a list of examples, in physical oceanography and large-scale air-sea interactions, that illustrate the science requirements for scatterometer systems in support of furthering our understanding of the Earth climate, and facilitating the development of useful weather forecasts as well as climate predictions. This is by no means an exhaustive list of examples. Surface vector wind data are also relevant to issues in climate and operational domains not dealt with here, *e.g.* atmospheric chemistry, the global water cycle, mesoscale meteorology, ice dynamics, *etc.* We fully anticipate scientific advances in these areas with the rapid growth of the surface vector wind database in the coming decade.

The discussion is organized as follows. In section 6.1 we examine the role of high-frequency and high-wavenumber wind forcing in mid-latitude and tropical mixing events in the upper ocean and the feedback onto the climate system. Features of the global wind-stress curl field are discussed in section 6.2. Surface vector wind representations of ENSO are described in section 6.3. The surface vector wind requirements of modern regional and global ocean models are discussed in section 6.4.

6.1 - Global SST Annual Cycle; Amplitude and Phase

The sea-surface temperature (SST) modulates fluxes of sensible and latent heat, longwave radiation, and fresh water across the air-sea interface. From a global perspective, these exchanges form a major part of the thermodynamical component of the Earth climate. The thermodynamics are coupled to the dynamics through convection and mixing processes in the boundary layers of the ocean and atmosphere. Vertical mixing and convection in the upper ocean are processes that exemplify the notion of climate as the integral effect of interacting large-amplitude events. In this section we describe upper ocean dynamics driven by the surface wind field, that determine the seasonal signal of SST over broad regions of the mid-latitude and equatorial oceans.

6.1.1 - *Inertial Resonance and the Ocean Mesoscale Eddy Field*

The dominant forcing effect of the surface wind on the upper ocean in mid-latitudes is particularly large in autumn when the ocean response is confined from below by a strong seasonal thermocline, and atmospheric storm intensities and frequencies are increasing. It is observed in this season that, despite a net heat flux into the ocean, the upper ocean is cooling on average (Large *et al.*, 1986). This large-scale cooling results from mixing of colder deeper waters into the upper ocean. Large-amplitude episodic cooling events have been observed in the upper ocean under these conditions, associated with the passages of storms. Sea-surface temperature changes can be as large as 1°C in *6 hr*, requiring more than $1000 Wm^{-2}$ of cooling. In addition, there are observations of significant perturbations in depth (deeper) and temperature (warmer) of the seasonal thermocline which can have ramifications for the ocean general circulation.

Interestingly, episodic cooling events are associated with some, but not all storms. The horizontal spatial scales of the observed coolings are between 50*km* and 200*km* at middle latitudes. Large and Crawford (1995), and Crawford and Large (1996) demonstrate that episodic cooling is the signature of a resonant interaction between the surface wind stress and inertial circulations in the upper ocean.

As much as *70%* of the seasonal change in mid-latitude SST occurs in *10%* of the strong forcing events via this mechanism (Large *et al.,* 1986).

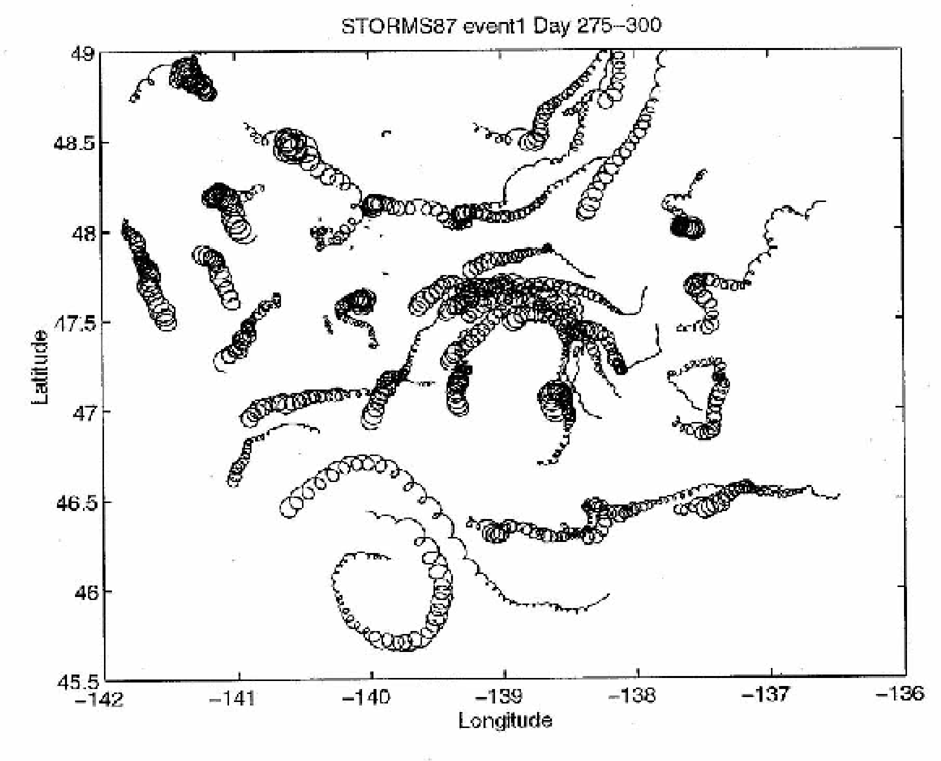

Figure 4. Drifter tracks during the Ocean Storms Experiment exhibiting inertial currents in the upper ocean (Adapted from D'Asaro *et al.* (1995); courtesy P. Niiler).

Figure 4 is an example of inertial currents as detected by surface drifters during the Ocean Storms Experiment (D'Asaro *et al.,* 1995). The inertial eddy circulation time, or inertial period, is a function of the local pendulum day; *i.e.,* latitude. The inertial period at 45° latitude is 18*hr*. When the surface wind vector rotates in synchrony with the inertial currents in the surface ocean (*i.e.,* resonates in space and time), then vertical mixing in the upper ocean is exponentially deeper than in more common instances of surface forcing that are asynchronous with respect to local inertial oscillations. Lee *et al.,* (1994) account for contributions from the ocean mesoscale eddy field to this process (*i.e.,* a doppler shift effect to be combined with inertial oscillations in the upper ocean circulation). The passages of atmospheric fronts in the mid-latitudes can provide appropriate time and space scales for inertial resonance in the upper ocean.

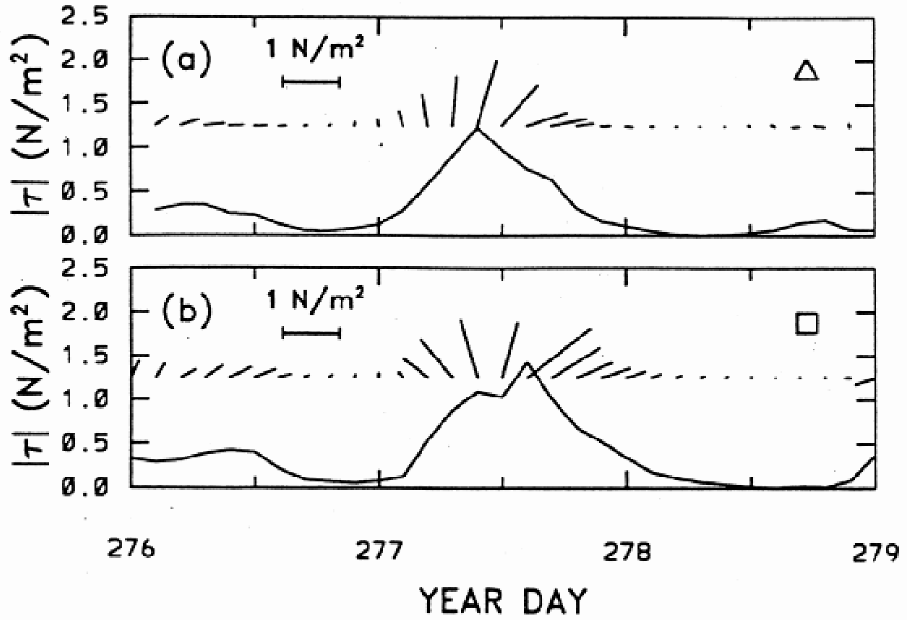

Figure 5. Wind stress intensity and direction as functions of time at 2 locations (**a** and **b**) separated by about 200*km* during the Ocean Storms Experiment (adapted from Large and Crawford, 1995).

Figure 5 demonstrates the passage of such a storm over two drifting buoys (denoted **a** and **b**) separated by about 200*km* during the Ocean Storms Experiment. The two panels depict the wind stress intensities and directions as functions of time at positions **a** and **b**. Surface wind stress intensity (solid line) peaks before noon on year day 277 at location **a**, and just after noon at location **b**. The time histories of direction and amplitude of the surface wind stress vectors (stick plots) are also shown. As the storm intensifies and propagates through the region, the wind stress vector rotates 180° in fewer than 24*hr*, consistent with the local inertial period.

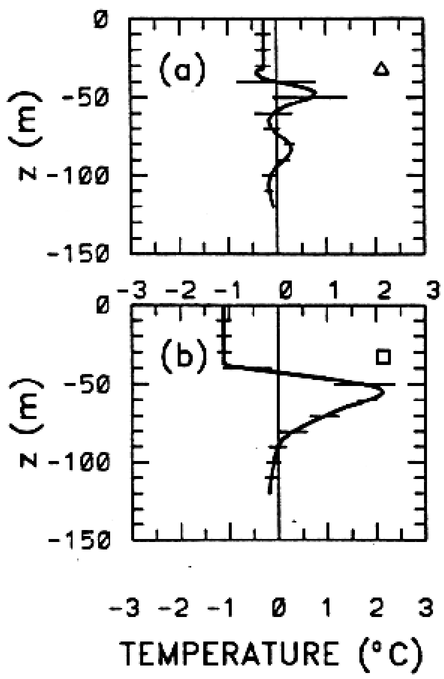

Figure 6. Upper ocean temperature profile change at locations **a** and **b** for the time period associated with the storm depicted in Fig. 5. The surface wind stress is in near-inertial resonance with the upper ocean at **b**, and not so at location **a** (adapted from Large and Crawford, 1995).

The two panels in Fig. 6 demonstrate the upper ocean mixing responses (temperature differences *vs.* depth). At location **a** the temperature perturbations are smaller than or equal to *1°C* over all depths. At location **b**, the wind stress rotates in synchrony with the local inertial currents and the temperature perturbation profile characteristic of the episodic cooling process is evident (bottom panel). The upper *50m* cool by more than *1°C*, and the thermocline region warms (up to *2°C*) and diffuses below *50m* depth. A third drifting buoy separated from location **b** by about 50*km* exhibited a similar response. Thus an estimate of the spatial scale of variability for the inertial resonance phenomenon in the North Pacific is larger or equal to 50*km*, but shorter than 200*km* (*i.e.*, location **a**). Syntheses of the regional observations over the course of the Ocean Storms Experiment demonstrate a *50%* deepening of the seasonal thermocline associated with the inertial resonance process.

Therefore;

- Inertial temporal and spatial scales in the surface vector wind field must be resolved in mid-latitudes in order to quantify the impacts of episodic deep mixing events that set the amplitude and phase of the seasonal cycle in SST, and thus the air-sea fluxes of momentum, heat, longwave radiation, and moisture over most of the mid-latitude world ocean.

6.1.2 - *Diurnal Effects on Seasonal SST at the Equator*

The seasonal air-sea heat flux at the equator is of obvious climatic importance. Theories for the triggering of ENSO warm events depend sensitively upon the build-up of ocean temperatures in the western Pacific warm pool. Atmospheric deep convection, the upward branch of a large-scale poleward heat transport process, is sensitive to the surface heat flux on timescales from hourly, to intra-seasonal, to interannual. Ocean uptake and storage of heat supplied by the atmosphere during day light hours at the equator is a process that depends on precise synchrony between the diurnal heating cycle and strong vertical mixing in the upper ocean.

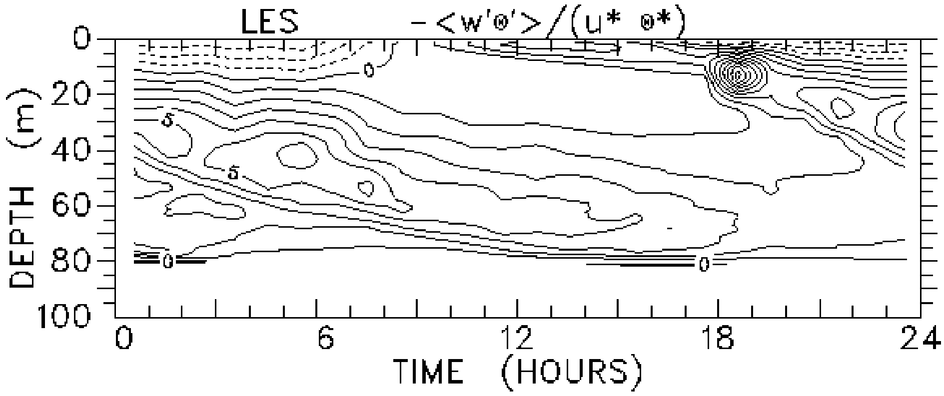

Figure 7. The diurnal cycle of heat flux plotted as a function of depth and normalized by $u^*\theta^* = 1.5 \times 10^{-5}\ m\ s^{-1}\ K$. The surface forcing repeats every *24 hr* so that the righthand edge of the figure blends in time with the lefthand edge (adapted from Large and Gent, 1999).

Figure 7 demonstrates the normalized vertical mixing of potential temperature in a large-eddy simulation of the upper 100*m* of the equatorial ocean. Daytime surface heating stratifies the upper ocean at the equator, trapping excess momentum near the surface. The daily excess of momentum can be viewed as a near-surface distortion of the linear vertical shear profile that spans the upper ocean from the surface to the core of the equatorial undercurrent at about 100*m* depth. Night time cooling at the surface stimulates convection (18:30 hours in Fig. 7) that penetrates the shallow stratification, mixing in the vertical the heat and momentum that were trapped near the surface during the day. The mixing occurs as local Richardson numbers approach critical values at progressively deeper levels down the vertical shear profile. The local mixing in the vertical pumps heat downward, penetrating eventually to 80*m* during the following day, while the heat and momentum storages in the surface layers begin to rebuild.

Large and Gent (1999) document a parameterization of vertical mixing in the upper ocean that captures the diurnal mixing in the vertical at the equator. The set-up of the background vertical shear profile, and the extent of the diurnal mixing in the vertical depend critically upon momentum inputs to the upper ocean from surface winds at the equator.

Therefore;

- The diurnal cycle of momentum input to the ocean at the equator must be resolved in order to quantify seasonal fluxes of heat and momentum.
- Accurate zonal winds across the entire equatorial basin are required to estimate the equatorial undercurrent strength and hence the upper ocean vertical shear.

6.2 - Wind-Stress Curl

The curl of the surface wind stress is a critical vorticity source in the balances that describe the ocean general circulation. Away from western boundaries, the zonal integral of the wind-stress curl defines the Sverdrup streamfunction describing the sub-tropical and sub-polar gyre circulations of the world ocean. The integral effect in the vertical of Ekman divergences, driven directly by the wind-stress curl, is a stretching of vortex tubes throughout the fluid that must be compensated by a translation in latitude. This leads to Rossby wave propagation and basin-scale adjustment processes. In mid-latitude coastal domains, along ocean eastern boundaries, wind-stress curl extrema are indicative of coastal upwelling centers and associated biological productivity (Nelson, 1977; Bakun and Nelson, 1991). Persistent boundary wind-stress curl features have recently been associated with the morphology of sub-tropical gyre circulations (Milliff *et al.*, 1996). We review the climate scale implications wind-stress curl in the coastal and open ocean. The long-term average wind-stress curl from NSCAT is shown to be affected by artifacts over the open ocean associated with incomplete sampling of large-amplitude storm events (Milliff and Morzel, 2000).

6.2.1 - *Wind-Stress Curl in the Coastal Ocean*

Equatorward surface winds, and lateral shears in the atmosphere intensify on seasonal and synoptic timescales near eastern boundaries of the world ocean. This forcing induces an offshore mass flux in the upper ocean that is compensated near the coast by vertical fluxes of nutrient-rich, colder waters from depth. The offshore scale of these coastal upwelling centers is on the order of a few first-baroclinic mode Rossby radii of deformation; $O(10^2 km)$. The upwelling events are episodic with life cycles of 3 to 5 days. Cold, nutrient-rich surface waters have obvious implications for ocean biota from the effects on organisms relevant to primary productivity, to the commercial productivity of coastal fisheries. In addition, the cold surface waters near the coast modulate air-sea interactions and are implicated in the production of marine stratus clouds that in turn affect the radiative equilibrium of the atmospheric boundary layer on seasonal timescales (Kiehl *et al.*, 1998).

Therefore;

- The temporal (sub-daily) and spatial (50*km*) scales of the wind forcing that drive the coastal ocean upwelling response should be resolved in order to quantify effects on seasonal air-sea heat flux, as well as a large seasonal signal in biological productivity.

Figure 8 depicts the nine-month average wind-stress curl from 25*km* NSCAT data binned to 0.5° (left most), 1° (middle left), and T62 (middle right) resolutions. The right most panel is the nine-month average wind-stress curl computed from the 10*m* winds from the NCEP analyses at T62, for the same time period (Milliff and Morzel, 2000). For the left most panel in Fig. 8, the wind-stress curl average is computed by: binning the 25*km* NSCAT wind retrievals into 0.5° bins, computing stress components for each wind observation, averaging stress components within each bin, and computing curl using the smallest natural spatial stencil. This procedure is applied orbit-by-orbit so as not to compute curl from binned stress values from widely different times. Given the spatial derivative operation inherent in the wind-stress curl calculation, half-degree bins are near the high-resolution limit for the 25*km* NSCAT observations. The orbit-by-orbit wind-stress curl is accumulated and averaged over the lifetime of the NSCAT mission. The narrow cross-shore spatial scales of wind-stress curl features off California, Baja California, Peru and Chile are the time-average manifestations of eastern boundary wind-stress curl features first described by Nelson (1977). Similar features occur off southern and northwestern Africa (not shown). The boundary wind-stress curl amplitudes are markedly higher, and often of opposite sign *vs.* wind-stress curl in adjacent offshore regions.

We can repeat the nine-month average wind-stress curl calculation from NSCAT data this time using 1° bins to aggregate the wind retrievals. Remarkably, the eastern boundary wind-stress curl features have all but disappeared in this aggregation of the NSCAT data (middle-left panel). We can aggregate the NSCAT data to still coarser resolution, this time employing T62-resolution bins consistent with NCEP analyses. The middle right panel is the nine-month average wind-stress curl field constructed from NSCAT data in this way, and the right most panel is the comparable field from the NCEP analyses. Not surprisingly, the narrow eastern boundary wind-stress curl features in the NSCAT data (left most panel) are eradicated completely at T62 resolution (middle right).

There are significant differences in the distribution of time-average wind-stress curl evident in the two righthand panels of Fig. 8. Notable coastal features in the right most panel from the NCEP analyses might be confused with the eastern boundary wind-stress curl features of interest. However, inspection of the global fields (not shown) reveals that the coastal features in the NCEP wind-stress curl need not occur on ocean eastern boundaries (*e.g.*, off China), and that the along- and across-shore scales of the features in NCEP wind-stress curl (right most) are large compared to eastern boundary features in wind-stress curl from NSCAT at 0.5° resolution. Further, the signs of the boundary wind-stress curl features from NCEP do not all agree with features along the same boundaries in the NSCAT fields (*e.g.*, see the Drake Passage, Fig. 8).

The boundary wind-stress curl features in the NCEP analyses are not the coarse-resolution representation of a geophysical signal at all. They result from the effects of wavenumber truncation in the spectral models used to produce the weather-center forecasts and analyses. In these models, the surface geopotential height field over the ocean is supposed to be a flat field with amplitude $\Phi = 0$. However because of spectral truncation, transitions from tall coastal topography to the flat sea surface cannot be faithfully represented. Instead, the model geopotential surface overshoots and oscillates about $\Phi = 0$, with a peak-to-peak spatial scale that is a function of the spectral resolution and the size of the topographic transition. The Andes pose a particularly large topographic transition and the amplitude of the overshoot in surface geopotential is more than *200 m* in the near-coastal ocean there.

This is a well-known property of spectral models and the oscillations are referred to as "Gibbs phenomena" or "spectral ringing." Spectral ringing artifacts in the surface geopotential contaminate the 10*m* wind forecasts and analyses since the surface winds are proportional to spatial gradients in the geopotential surface. The spectral ringing is a permanent artifact in near-coastal ocean regions.

Thus, the eastern boundary wind-stress curl extrema that begin to appear in fields derived from 25*km* resolution surface vector wind data, occur in the regions of the largest amplitude aliasing in analysis field outputs from spectral forecast models. In this sense, the only reliable source of observations of this climatically important signal is high-resolution space-borne scatterometer data.

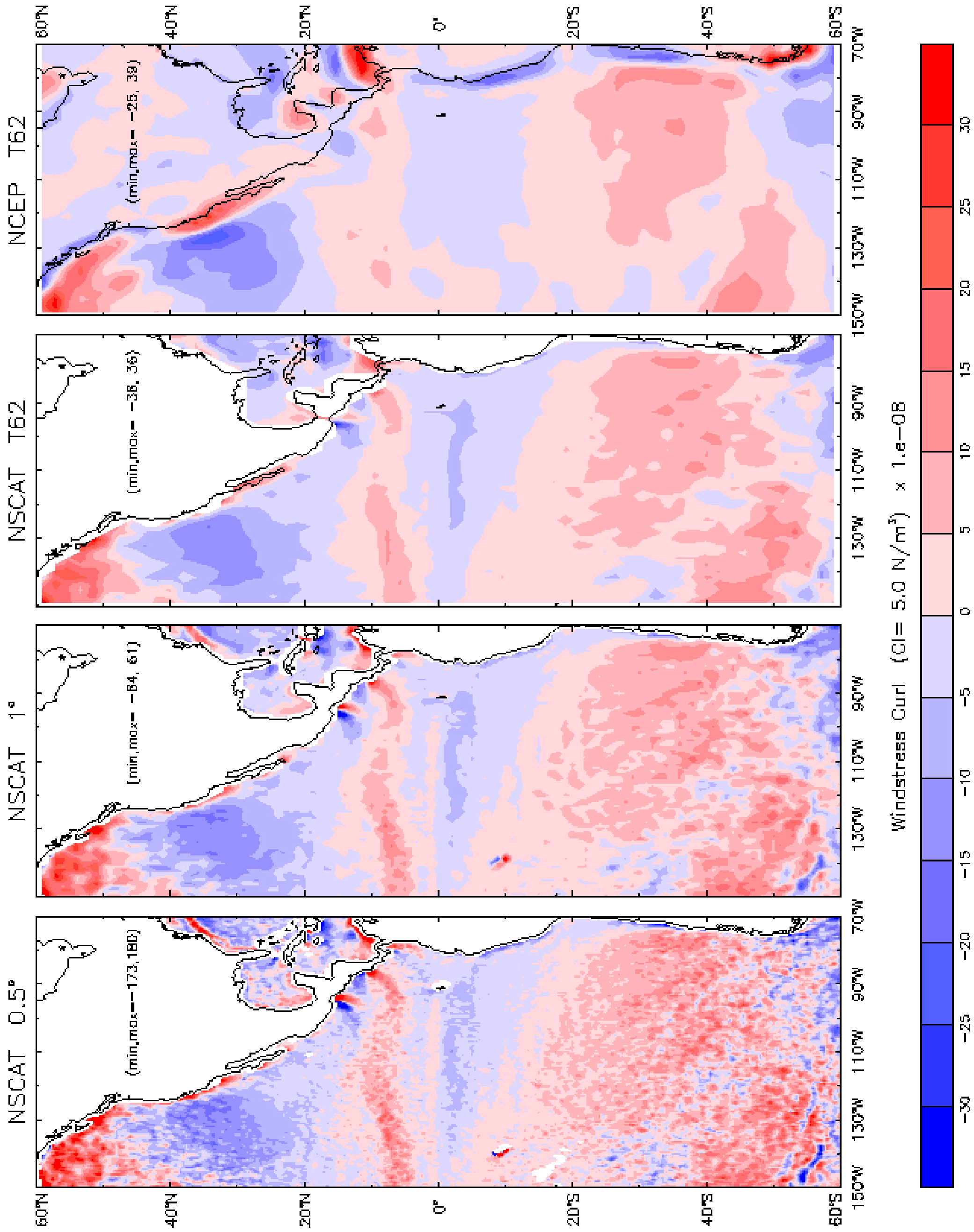

Figure 8. Nine-month Average Wind-Stress Curl from NSCAT data binned to *0.5°* (left most), 1° (middle left), and T62 (middle right) resolutions. The right most panel is the comparable average wind-stress curl from the T62 NCEP analyses (adapted from Milliff and Morzel, 2000).

Therefore;

- The narrow cross-shore scale (50*km*) of persistent eastern boundary wind-stress curl features must be resolved to quantify vorticity inputs that affect the morphology of sub-tropical gyre circulations in the ocean.

6.2.2 - *Wind-Stress Curl over the Open Ocean*

We can review Figs. 8 with regard to the wavenumber content of the wind-stress curl field over the open ocean as well. A mesoscale patchiness is obvious at the highest resolution (left most panel), that is not at all evident in the field derived from NCEP analyses (right most panel). The middle panels are consistent with larger-scale averages of the patchiness at 0.5° resolution (*e.g.* see Southern Ocean).

Milliff and Morzel (2000) show that the patchiness is an artifact of incomplete sampling of propagating large-amplitude storm events in the time-dependent wind-stress curl field over the ocean. While our intuition might be well developed for the variability of high-amplitude winds associated with atmospheric storms, the wind-stress curl is geometrically more variable in space and time.

This implies that a single, broad-swath scatterometer system such as NSCAT is not sufficient to resolve climatically important vorticity inputs to the ocean. To do so requires resolution of the wind-stress curl decorrelation time associated with these events. This is a quantity that has yet to be measured on synoptic scales. However, the NSCAT data provide evidence of previously undetected high frequency variability or intermittency of the global wind-stress curl field (D. Chelton, personal communication).

Animations of the wind-stress curl computed from NSCAT in the inter-tropical convergence zone (ITCZ) of the eastern Pacific demonstrate highly intermittent features of narrow meridional scale (50*km*) and large zonal scale (1000*km*), with opposite signed vorticity (positive to the north of the ITCZ, and negative to the south) bounding the region of atmospheric deep convection. The timescales for the appearance and total disappearance of these features is on the order of 1 day (Chelton *et al.*, 1999). Vestiges of this variability remain in the highest resolution nine-month average in Fig. 8 (left most panel).

Therefore;

- Co-ordinated, multiple, space-borne scatterometer systems are required to resolve the intermittency in the wind-stress curl associated with the propagation of atmospheric storms.

6.3 - ENSO

One of the major motivations of the Tropical Ocean and Global Atmosphere (TOGA) Coupled Ocean-Atmosphere Response Experiment (COARE) is to fill in physics missing from most prediction models of the El Nino Southern Oscillation (ENSO). Prominent among these missing elements is the Madden-Julian Oscillation (MJO; Madden and Julian, 1971). Lau (1985) first postulated that the MJO can influence and trigger ENSO. Nakazawa (1988) showed that the active phase of the MJO contains a hierarchy of convection, including cloud clusters, as it propagates from the Indian Ocean into the western Pacific, where ENSO events can be triggered. The MJO generates westerly wind bursts which usually last for a few days, in the western equatorial Pacific over the warm pool (*e.g.* Luther *et al.*, 1993). The westerly wind bursts are believed to force Kelvin waves that have been associated with warming in the east (*e.g.* Lukas *et al.*, 1984). While equatorial moorings may be able to monitor high-frequency wind forcing at a few locations near the equator, Liu *et al.* (1996) demonstrated that realistic off-equatorial forcing is important in the simulation of ENSO changes with ocean general circulation models (OGCM). Sufficient areal wind coverage has to rely on space-based data. Liu *et al.* (1995), using surface wind vector observations from space-borne platforms, was able to link surface wind forcing to observed propagation of Kelvin waves across the Pacific, that coincided with the onset of an ENSO warm event. They also simulated successfully the equatorial warming with an OGCM forced by scatterometer winds. Since TOGA COARE, the role of MJO in ENSO has been revealed in observations and model simulations (*e.g.* Picaut and Delcroix, 1995; Kessler *et al.*, 1995; Vialard and Delecluse, 1998). The role of westerly wind bursts in the ENSO teleconnection was also demonstrated with high-resolution wind data from NSCAT by Liu *et al.* (1998).

6.4 - Surface Vector Wind Requirements for Ocean Numerical Models

Recent theoretical and algorithmic advances of two kinds have resulted in numerical ocean model simulations that are in better agreement with ocean observations than was the case just a few years ago. This statement is true for two distinct classes of ocean numerical models; the highest-resolution basin-scale models, as well as the coarser resolution global ocean general circulation models (OGCM). The conceptual and numerical advances leading to these breakthroughs have to do with: the parameterization (*e.g*, Gent *et al.*, 1995) and/or resolution (*e.g.*, Bryan and Smith, 1998) of mesoscale eddies; and the switch from traditional relaxation or restoring forms for ocean surface boundary conditions, to bulk flux forms (Large *et al.*, 1997).

Clearly, both areas of improvement are closely related to the surface vector wind forcings imposed on the models of both classes. The parameterization of mesoscale eddies and associated mixing processes raises the classical question of direct vs. indirect forcing of the ocean mesoscale eddy field by the surface wind. Bulk flux surface boundary conditions for momentum (and therefore kinetic energy input) depend upon surface vector wind information. Surface boundary conditions of bulk-flux form for thermodynamic variables depend upon surface wind speed information.

Ocean numerical model sophistication has reached a stage that permits comparisons of the ocean responses to changes in surface boundary conditions where the interpretations of model results are not as ambiguous with respect to partitioning ocean response signal from numerical artifacts and/or model deficiencies. It is now the standard for basin-scale model and OGCM comparisons with data, that snapshots from particular times be well-matched between model and data (*e.g.*, Spall *et al.*, 1999). Similarly, comparisons of average properties between model output and observational climatologies must also match, as closely as possible, in the temporal and spatial scales inherent in the respective averages.

These new standards for comparison impose more stringent requirements on the vector wind forcing data sets than has been the case until now. In this sub-section we explore the implications of two recent examples of ocean numerical experiments with regard to issues of surface vector wind forcing.

6.4.1 - *High-Resolution Basin-Scale Models*

For most of the relatively brief history of ocean numerical modelling, it has been the case that basin-scale, three-dimensional, primitive equation (3DPE) ocean simulations have not matched well with details apparent in ocean observations. The history of 3DPE ocean modelling is longest, and perhaps most highly developed for models of the Atlantic Ocean basin. Until recently, even at the highest affordable resolutions, 3DPE simulations of important features of the general circulation in the Atlantic were absent or poorly represented; including Gulf Stream separation, recirculation regions, and regional statistics dependent upon dynamics and energetics of the mesoscale eddy field (*e.g.*, poleward heat transport, mean and eddy kinetic energy distributions). Recently, a resolution barrier has been overcome such that the quality of the highest-resolution 3DPE simulations of the

North Atlantic are significantly better. In this section we highlight results from a 0.1° resolution calculation for the Atlantic Basin between 20°S and 73°N that are described in Bryan and Smith (1998) and Smith *et al.* (1999). The interested reader is referred to those manuscripts for details of the simulation. The main points here are: 1) the simulation is indeed a marked improvement over prior calculations at slightly coarser resolutions; and 2) given the capability to simulate realistically the mesoscale eddy field, we require high-quality surface vector wind forcing to address key issues of ocean general circulation theory.

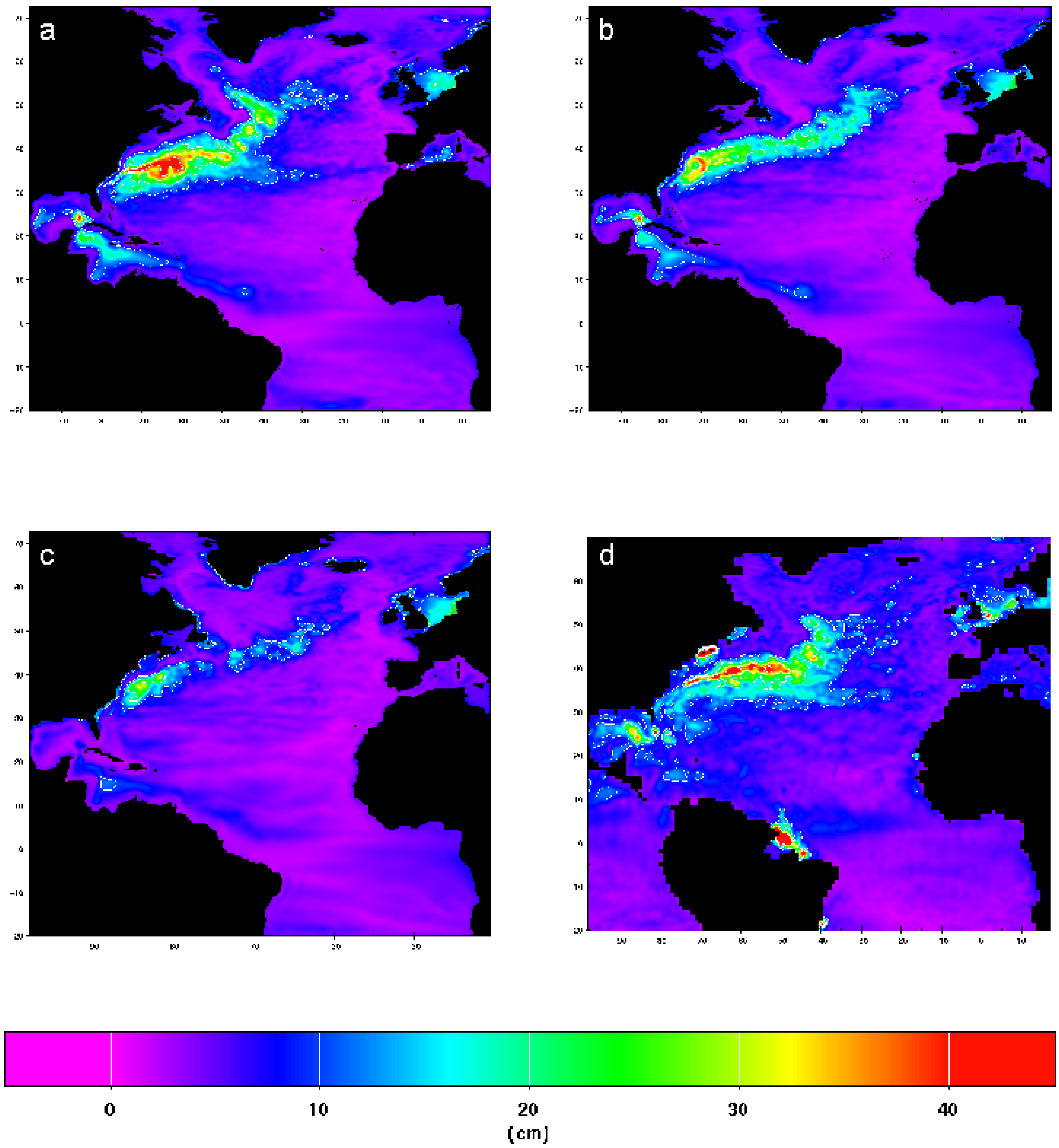

Figure 9. RMS sea surface height variability of North Atlantic numerical ocean models at **a)** *0.1°*, **b)** *0.2°*, **c)** 0.4°, and **d)** for a blended synthesis of altimeter data (LeTraon and Ogor, 1998) (this figure from Bryan and Smith, 1998).

Figure 9a-d (from Bryan and Smith, 1998) compares the RMS sea-surface height (SSH) variability from North Atlantic simulations at; a) 0.1°; b) 0.2°; and c) 0.4° with d) the altimeter-based estimates from Le Traon and Ogor (1998). While there are still systematic differences having to do with the dynamics of the free jet portion of the Gulf Stream, the simulation at 0.1° is clearly more faithful to the observations. In particular, the amplitudes and spatial scales of the SSH variability in the vicinities of the North Atlantic Current (50°N) and the Azores Current (35°N) are in very good agreement with the observations. The 0.1° 3DPE model simulation has been forced with daily winds interpolated from ECMWF analyses for the period 1985 through 1996.

The surface winds from weather-center analyses lack sufficient power in high-wavenumbers (Milliff *et al.,* 1996; Milliff *et al.,* 1999). Conversely, 25*km* resolution surface wind data (*e.g.,* ASCAT, NSCAT) permits three to four wind vector retrievals per mesoscale eddy diameter in the region of the North Atlantic current. The number of wind vector retrievals per eddy diameter doubles for SeaWinds class instruments. At higher latitudes (*e.g.*, the Labrador Sea) the eddy-sampling becomes more limited as the first-baroclinic mode Rossby radius of deformation, and therefore the local mesoscale eddy diameters, are smaller. Nonetheless, we can anticipate a capability for more accurate estimates of the correlations between eddy structures in the ocean and the observed circulations in the wind field. The potential to observe from simulations the dynamics of the forcing and response of the ocean mesoscale eddy field represents a significant milestone in the development of physical oceanography. Given anticipated advances in the resolution and coverage in altimetry, a validation dataset should also be available.

Therefore;

- The surface vector wind field should be observed on time and space scales, and over sufficient areas, so as to capture the forcings that correlate with the mesoscale eddy field in the ocean response.

6.4.2 - *Ocean General Circulation Models (OGCM)*

OGCMs have been forced with a repeat annual cycle of wind forcing based on the 9.5 months of NSCAT data, with ERS-2 scatterometer data used to fill in the remaining 2.5 months of a full year (*i.e.* the "NSCAT year" from August 1996 through July 1997; Milliff *et al.*, 1999). Companion integrations have used repeat 40 year cycles of NCEP reanalyzed winds, 1958 through 1997. Neither forcing is satisfactory. Problems with the latter include accuracy, spatial and temporal variability and consistency, as discussed above. However, a very important result of these NCEP solutions is that many of the simulated years show the sub-polar gyre of the North Atlantic extending southward along the eastern coast of the U.S. into the Middle Atlantic Bight. This feature is extremely important climatically, because it keeps the warm waters of the Gulf Stream to the south where they belong. Without this southward penetration, the Gulf Stream travels too far north along the coast where its warm waters encounter a cold dry atmosphere, resulting in large and erroneous air-sea interaction.

Analysis of the NCEP forced solution for the NSCAT year shows a very strong sub-polar gyre, keeping the Gulf Stream near its proper position. However, the repeat NSCAT year forcing gives a very different result; the Gulf Stream travels far to the north, right along the coast. An interpretation of these results is that a long time history of forcing is required in order to model sub-polar, sub-tropical gyre interactions. We hypothesize that the whole sequence of wind-generated Rossby waves, especially those generated along the ocean eastern boundary, and westward propagation across the basin has important climatic effects on the western boundary current structure. At a minimum, both the barotropic and first baroclinic Rossby waves are likely to be important. The long time scale is set by the latter, at about 5 years for the North Atlantic basin.

Therefore;

- The surface vector wind field must be observed accurately, and consistently over a length of time comparable to the basin-scale transit time for the first baroclinic mode Rossby wave.

ACKNOWLEDGEMENT

The authors thank Frank Bryan, Dudley Chelton, and Peter Niiler for providing useful conversations, and figures used in this paper. The authors are members of the NSCAT Science Working Team, and they acknowledge NASA research support received in that capacity through the Jet Propulsion Laboratory. We thank Ms. B. Ballard and Ms. E. Rothney for their assistance in preparing this document.

REFERENCES

[Atlas 99] R. Atlas, S.C. Bloom, R.N. Hoffman, E. Brin, J. Ardizzone, J. Terry, D. Bungato, and J.C. Jusem: "Geophysical Validation of NSCAT winds using atmospheric data and analysis", *J. Geophys. Res. Oceans,* **104**, 11405-11424, 1999.

[Atlas] R. Atlas, and R.N. Hoffman: "The use of satellite surface wind data to improve weather analysis and forecasting", To appear in *Satellites, Oceanography, and Society*, Elsevier Science, Ltd.

[Bakun 91] A. Bakun, and C.S. Nelson: "The seasonal cycle of wind-stress curl in subtropical eastern boundary current regions", *J. Phys. Oceanog.,* **21**, 1815-1834, 1991.

[Bryan 98] F.O. Bryan, and R.D. Smith: "From eddy-permitting to eddy-resolving", *Intl. WOCE Newslet.,* **33**, 12-14, 1998.

[Chelton 99] D.B. Chelton, M.G. Schlax, J.M. Lyman, and R.A. de Szoeke: "The latitudinal structure of monthly variability in the tropical Pacific", *J. Phys. Oceanog.,* submitted., 1999.

[Chin 98] T.M. Chin, R.F. Milliff, and W.G. Large: "Basin-scale, high-wavenumber, sea-surface wind fields from a multiresolution analysis of scatterometer data", *J. Atmos. and Ocean. Tech.,* **15**, 741-763, 1998.

[Crawford 96] G.B. Crawford, and W.G. Large: "A numerical investigation of resonant inertial response of the ocean to wind forcing", *J. Phys. Oceanog.,* **26**, 873-891, 1996.

[D'Asaro 95] E.A. D'Asaro, C.C. Eriksen, M.D. Levine, P.P. Niiler, C.A. Paulson, and P. Van Meurs: "Upper-ocean inertial currents forced by a strong storm. Part I: Data and comparisons with linear theory" *J. Phys. Oceanog.,* **25**, 2909-2936, 1995.

[Gent 95] P. R. Gent, J. Willebrand, T.J. McDougall, and J.C. McWilliams: "Parameterizing eddy-induced tracer transports in ocean circulation models", *J. Phys. Oceanog.,* **25**, 463-474, 1995.

[Kessler 95] W.S. Kessler, M.J. McPhaden, and K.M. Weickmann: "Forcing of intraseasonal Kelvin waves in the equatorial Pacific", *J. Geophys. Res.,* **100**, 10613-10631, 1995.

[Kiehl 98] J.T. Kiehl, J.J. Hack, and J.W. Hurrell: "The energy budget of the NCAR community climate model: CCM3", *J. Climate,* **11**, 1151-1178, 1998.

[Large 86] W.G. Large, J.C. McWilliams, and P.P. Niiler: "Upper ocean thermal response to strong autumnal forcing of the northeast Pacific", *J. Phys. Oceanog.*, **16**, 1524-1550, 1986.

[Large 95] W.G. Large, and G.B. Crawford: "Observations and simulations of upper ocean response to wind events during the Ocean Storms Experiment", *J. Phys. Oceanog.*, **25**, 2831-2852, 1995.

[Large 97] W.G. Large, G. Danabasoglu, S.M. Doney, and J.C. McWilliams: "Sensitivity to surface forcing and boundary layer mixing in a global ocean model: Annual-mean climatology", *J. Phys. Oceanog.*, **27**, 2418-2447, 1997.

[Large 99] W.G. Large, and P.R. Gent: "Validation of vertical mixing in an equatorial ocean model using large eddy simulations and observations", *J. Phys. Oceanog.*, **29**, 449-464, 1999.

[Lau 85] K.M. Lau: "Elements of a stochastic dynamical theory of the long-term variability of the El Nino/Southern Oscillation.", *J. Atmos. Sci.*, **42**, 1552-1558, 1985.

[Lee 94] D-K. Lee, P.P. Niiler, A. Warn-Varnas, and S. Piacsek: "Wind-driven secondary circulation in ocean mesoscale", *J. Mar. Res.*, **52**, 371-396, 1994.

[Le Traon 98] P.-Y. Le Traon, and F. Ogor: "ERS-1/2 orbit error improvement using TOPEX/POSEIDON: the 2cm challenge", *J. Geophys. Res.*, **103**, 8045-8057, 1998.

[Liu 95] W.T. Liu, W. Tang, and L.L. Fu: "Recent warming event in the Pacific may be an El Nino", *EOS Trans of Amer. Geophys. Union*, **76**, 429-437, 1995.

[Liu 96] W.T. Liu, W. Tang, and R. Atlas: "Responses of the tropical Pacific to wind forcing as observed by spaceborne sensors and simulated by model", *J. Geophys. Res.*, **101**, 16345-16359, 1996.

[Liu 98] W.T. Liu, W. Tang, and H. Hu: "Spaceborne sensors observe various effects of anomalous winds on sea surface temperatures in the Pacific Ocean", *EOS Trans of Amer. Geophys. Union*, **79**, 249 and 252, 1998.

[Lukas 84] R. Lukas, S. Hayes, and K. Wyrtki: "Equatorial sea level response during the 1982-83 El Nino", *J. Geophys. Res.*, **89**, 10425, 1984.

[Luther 83] D.S. Luther, D.E. Harrison, and R.A. Knox: "Zonal wind in equatorial Pacific", *Science*, **222**, 237, 1983.

[Madden 71] R.A. Madden, and P.R. Julian: "Detection of a 40-50 day oscillation in the zonal wind in the tropical Pacific", *J. Atmos. Sci.*, **28**, 702-708, 1983.

[Milliff 96] R.F. Milliff, W.G. Large, W.R. Holland, and J.C. McWilliams: "The general circulation responses of high-resolution North Atlantic ocean models to synthetic scatterometer winds", *J. Phys. Oceanog.*, **26**, 1747-1768, 1996.

[Milliff 99] R.F. Milliff, W.G. Large, J. Morzel, G. Danabasoglu, and T.M. Chin: "Ocean general circulation model sensitivity to forcing from scatterometer winds", *J. Geophys. Res. Oceans*, **104**, 11337-11358, 1999.

[Milliff 00] R.F. Milliff, and J. Morzel: "The global distribution of time-average wind-stress curl from NSCAT", in preparation, 2000.

[Nakazawa 88] T. Nakazawa: "Tropical super cluster within intraseasonal variations over the western Pacific", *J. Meteor. Soc. Japan*, **66**, 823-839, 1988.

[Nelson 77] C.S. Nelson: "Wind stress and wind-stress curl over the California Current", *NOAA Tech. Rpt. NMFS SSRF-714,* U.S. Dept. of Commerce, 87pp., 1977.

[Picaut 95] J. Picaut, and T. Delcroix: "Equatorial wave sequence associated with warm pool displacements during the 1986 El Nino-La Nina", *J. Geophys. Res.*, **100**, 18893-18908, 1995.

[Smith 99] R.D. Smith, M.E. Maltrud, F.O. Bryan, and M.W. Hecht: "Numerical simulation of the North Atlantic ocean at 0.1 degree", submitted to *J. Phys. Oceanog.*, 1999.

[Spall 99] M.A. Spall, R.A. Weller, and P. Furey: "Modelling the three-dimensional upper ocean heat budget and subduction rates during the Subduction Experiment", *J. Phys. Oceanog.*, submitted, 1999.

[Vialard 98] J. Vialard, and P. Delecluse: "An OGCM study for the TOGA decade: Barrier-layer formation and variability", *J. Phys. Oceanogr.*, **28**, 1071-1106, 1998.